J Infrared Milli Terahz Waves (2015) 36:1182–1194
DOI 10.1007/s10762-015-0194-0

Parallel-Plate Waveguide Terahertz Time Domain Spectroscopy for Ultrathin Conductive Films

M. Razanoelina [1] · R. Kinjo [1] · K. Takayama [1] · I. Kawayama [1] · H. Murakami [1] · Daniel M. Mittleman [1,2] · M. Tonouchi [1]

Received: 12 May 2015 / Accepted: 20 July 2015 /
Published online: 16 August 2015

Abstract Development of techniques for characterization of extremely thin films is an important challenge in terahertz (THz) science and applications. Spectroscopic measurements of materials on the nanometer scale or of atomic layer thickness (2D materials) require a sufficient terahertz wave–matter interaction length, which is challenging to achieve in conventional transmission geometry. Waveguide-based THz spectroscopy offers an alternative method to overcome this problem. In this paper, we investigate a new parallel-plate waveguide (PPWG) technique for measuring dielectric properties of ultrathin gold films, in which we mount the thin film sample at the center of the waveguide. We discuss a model of THz dielectric parameter extraction based on waveguide theory and analyze the response of thin films for both transverse magnetic (TM) and transverse electric (TE) waveguide modes. In contrast to other waveguide methods, our approach enables comparison of the material response with different electromagnetic field distributions without significantly changing the experimental setup. As a result, we demonstrate that TE modes have a better sensitivity to the properties of the thin film. For prototype test samples, optical parameters extracted using our method are in good agreement with literature values.

Keywords Thin conductive film · Parallel-plate waveguide · Terahertz

1 Introduction

Characterization of the electromagnetic properties of thin films has long been an important topic in spectroscopy. In recent years, this has become even more relevant with the growing

✉ M. Razanoelina
razanoelina@ile.osaka-u.ac.jp

[1] Institute of Laser Engineering, Osaka University, Suita, Osaka 565-0871, Japan

[2] Electrical and Computer Engineering Department, Rice University, 6100 Main St, Houston, TX 77005, USA

interest in two-dimensional materials including graphene, molybdenum disulfide (MoS_2), and other nanosheet materials [1–3]. In the terahertz (THz) range, such materials have been recognized as important building blocks for future optoelectronic devices [4, 5]. However, characterizing such extremely thin films using conventional THz spectroscopy is often challenging for several reasons. First and most obvious, the extreme subwavelength thickness offers a very limited interaction length in the conventional normal-incidence transmission geometry. As a result, only a very small, essentially unmeasurable change is induced by material. Second, fabricating films with atomic-scale uniformity over an area larger than the diffraction-limited focal spot of THz beam is very challenging in many cases [6].

Various alternative approaches have been demonstrated for the study of thin films using THz–time domain spectroscopy (TDS). These include attenuated total internal reflection (ATR) spectroscopy [7] and broadband near-field spectroscopy [8]. One approach of note is the use of waveguide-based spectroscopy pioneered by Grischkowsky and co-workers [9]. Here, a thin dielectric polycrystalline solid is deposited on one plate of metal parallel-plate waveguide (PPWG), providing a long interaction length and therefore high sensitivity to, e.g., vibrational absorption bands in polycrystalline films [10]. One disadvantage of this approach is that sensitivity depends on the thickness of the thin layer relative to waveguide plate spacing, so a very thin (e.g., less than 10 nm) layer would give rise to a tiny signal [11]. A more compelling problem is that the technique is unsuitable to the study of conductive layers, since the sample becomes essentially indistinguishable from the metal substrate.

Here, we describe a new waveguide-based approach which maintains the advantage of long interaction length between the thin film and the propagating THz wave, but which is suitable for conducting films. We still rely on the PPWG, but in our approach, the thin metal layer is situated half-way between the two metal waveguide plates, rather than in contact with one of them. In the earlier approach, the studies all made use of lowest order transverse magnetic mode (the TEM mode) of the waveguide, since the transverse electric (TE) mode amplitude vanishes at the metal plate surfaces (which eliminates the interaction with the sample). However, recent work has shown that TE modes can also prove useful for highly sensitive waveguide-based sensing [12, 13]. In this paper, we compare the response for both transverse magnetic and transverse electric excitation of the waveguide. Using a series of thin gold films exhibiting a thickness-dependent metal–insulator transition [14], we investigate the sensitivity of our approach and develop a formalism for extracting quantitative dielectric parameters of the thin film from our measurements. In the case of the odd TE modes (TE_1, TE_3, etc.), our sample is located at a maximum of the electric field, which optimizes the interaction between the electromagnetic wave and the sample. As result, we find that TE mode excitation gives results which are more sensitive to the dielectric properties of the thin film and are therefore in better agreement with the expected behavior of this prototype thin film system [14].

This paper is outlined as follows: The theory section gives the main expressions to extract dielectric parameters of conductive thin films in our approach. The next section describes the experimental setup used for PPWG-based THz–TDS and the sample preparation. In Section 3, we show the results obtained for four gold films of different thicknesses. Section 4 explains the difference between TE mode and transverse magnetic (TM) mode configurations in PPWG sensing for thin conductive film. Finally, the discussion section compares the PPWG method and normal transmission THz–TDS method, also performed during this work.

2 Theory

The mathematical approach for describing a thin slab centrally located inside a waveguide has been developed by many researchers. For example, in [15], a thin dielectric slab is centrally placed in a rectangular waveguide in order to measure its optical permittivity in the microwave range. Other analyses have been done for very thin resistive sheets inside a rectangular waveguide to suppress higher order mode propagation [16]. An exact formulation of a PPWG loaded with a thin material sheet has been also derived in [17] for TEM and TM_1 mode excitation. Here, our approach is based on two assumptions: (i) The sample under analysis is infinitely thin and characterized by a finite surface conductivity σ_s; (ii) Only TE (TM) modes are excited if the input beam has an electric fields parallel (perpendicular) to the thin film surface and the waveguide plates.

We consider an extremely thin conductive sheet symmetrically located in a PPWG as shown in Fig. 1a. The boundary conditions to be satisfied are $E_{tan}=0$ on the metallic walls and

$$E_{\tan,1} = E_{\tan,2}$$
$$n \times (H_2 - H_1) = J_S = \sigma_s E$$

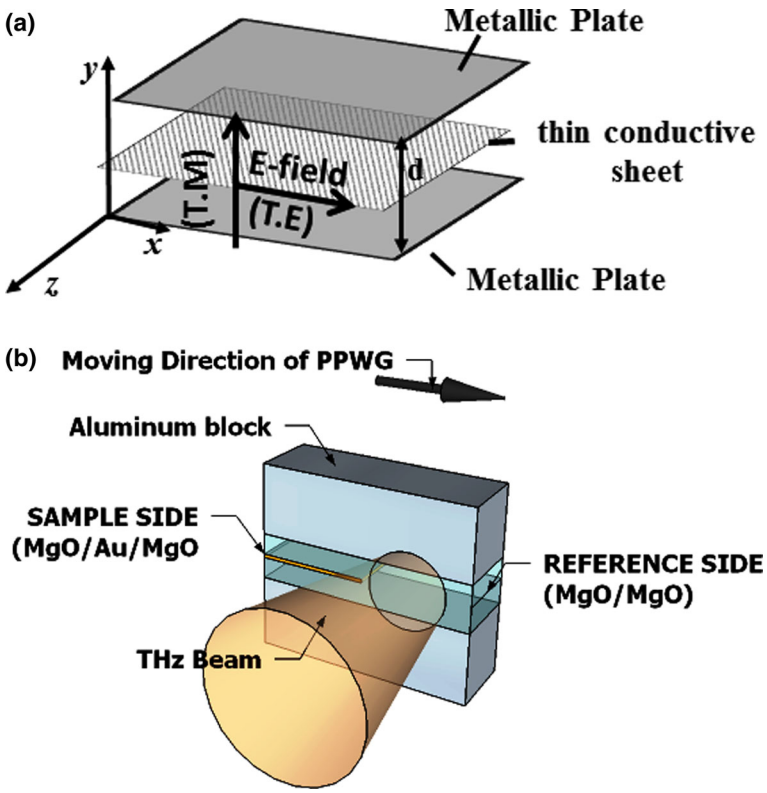

Fig. 1 **a** Ultrathin thin film of conductive material located at the center of PPWG with electric field orientation in TE mode and TM mode. **b** Reference (MgO/MgO) and sample (MgO/Au/MgO) side configuration in PPWG THz–TDS. The waveguide is moving perpendicularly to the THz beam propagation

at the conductive interface. J_s (A/m) is the surface current, E and H are the electric and magnetic fields, respectively, σ_s (units S) is the surface conductivity, and n is a unit vector normal to the film surface, pointing from the region 2 to region 1.

Without loss of generality, the electromagnetic fields can be divided into TE and TM fields. Taking into account of the above conditions as well as of the symmetry properties, the dispersion equations derived by solving Maxwell equations are [16]

$$\sigma_s \omega\mu = 2jk_y \cot\left(k_y \frac{d}{2}\right) \text{ for TE mode} \tag{1}$$

$$\sigma_s = \frac{2j\omega\epsilon}{k_y} \cot\left(k_y \frac{d}{2}\right) \text{ for TM mode} \tag{2}$$

Here, $k_y^2=\gamma^2+k^2$, where $k^2=\omega^2\epsilon\mu$ and $\gamma=j\beta+\alpha$ is the complex propagation constant along the z direction (coordinate system defined in Fig. 1a). β and α are the phase constant and the attenuation, respectively. d is the PPWG plate separation. In the extremely thin film approximation [18], $\sigma_s=\sigma t$ where σ is the volume conductivity and t is the thickness of the film. Eqs. (1) and (2) allow us to compute γ for given values of σ_s. Conversely, these equations will be used to estimate the value of σ_s.

In THz–PPWG sensing, the parameter extraction is generally based on the frequency-dependent transfer function for single-mode propagation [19]. This single-mode requirement is not always fulfilled especially in our case. With a 1-mm plate separation and a PPWG filled with dielectric as reference, higher order modes can propagate. Mendis et al. [20] have overcome this problem by mode matching of the lowest order TE_1 mode with the Gaussian incident beam. In that case, increasing the plate separation maintains an undistorted THz pulse propagation, if the incident beam's size also increases. However, in our case, the relatively large plate separation and the need to compare sample and reference with the same plate separation means that we will necessarily be exciting higher order modes.

We therefore apply a multimode transfer function to carry out the parameter extraction. The reference signal is the THz electric field detected through a waveguide containing only substrate and the sample signal is the electric field detected through waveguide containing a thin conductive film between the substrate:

$$T(\omega) = \frac{E_{\text{samp}}}{E_{\text{ref}}} = \frac{\sum_m t_{\text{in,samp},m} t_{\text{out,samp},m} C^2_{y,\text{samp},m} C_{x,\text{samp},m} e^{-j(\beta_m,\text{samp})L} e^{-\frac{\alpha_{m,\text{samp}}}{2}L}}{\sum_n t_{\text{in,ref},n} t_{\text{out,ref},n} C^2_{y,ref,n} C_{x,\text{ref},n} e^{-j(\beta_n,\text{ref})L} e^{-\frac{\alpha_{n,\text{ref}}}{2}L}} \tag{3}$$

All parameters in the above equation depend on the frequency and the mode. t_{in} and t_{out} are the transmission coefficients that include the impedance mismatch between the material inside the guide and free space. C_x and C_y are the coupling coefficients of the input field to the waveguide modes that can be calculated by the standard overlap integral [19]. β_m is a complex value computed from Eqs. (1) and (2), and α_m is the loss due to the finite conductivity of the waveguide plates [21].

For our procedure, THz pulse in free space could be used as the reference for the data processing described in this section. However, to avoid complicated calculation including the

diffraction loss and changes in the optical alignment during the optimization process, the parallel-plate waveguide filled with dielectric (but with no metal film) is taken as the reference. We note that the TEM mode is the fundamental TM mode, which has no cutoff frequency and no signal dispersion. In contrast, the fundamental TE_1 cutoff (and dispersion) depends on the filling media of the PPWG.

Once the reference signal is well defined, either for TM mode or TE mode, the optimization process is to numerically minimize the following error functions:

$$tER(\omega) = \left|T_{\text{exp}}(\omega)\right| - \left|T_{\text{theory}}(\omega)\right| \tag{4}$$

$$aER(\omega) = \varphi\left(T_{\text{exp}}(\omega)\right) - \varphi\left(T_{\text{theory}}(\omega)\right) \tag{5}$$

$$ER = \sum_{\omega} |tER(\omega)| + |aER(\omega)| \tag{6}$$

$$T_{\text{exp}}(\omega) = \frac{E_{\text{samp}}}{E_{\text{ref}}}. \tag{7}$$

Here, E_{ref} is the Fast Fourier Transform (FFT) of the reference signal and E_{samp} is the FFT of the sample signal. $T_{\text{theory}}(\omega)$ is the theoretical complex transfer function in Eq. (3). $tER(\omega)$ and $aER(\omega)$ are the error to minimize for the amplitude and for the phase, respectively.

The general Drude–Smith model is used for the conductivity of a thin gold film [22]:

$$\sigma = \frac{\epsilon_0}{(1 - j\omega\tau)}\,\omega_{\text{p}}^2\tau\left[1 + \frac{c}{(1 - j\omega\tau)}\right] \tag{8}$$

σ is the conductivity, ω is the angular frequency, τ is the scattering time, ω_{p} is the plasma frequency, ϵ_0 is the vacuum permittivity, and c is a parameter called "persistence of velocity" with $-1 \le c \le 0$ [14]. If $c=0$, the conductivity is the classical Drude model. If $c=-1$, all carriers are localized.

In the error minimization, the parameters ω_{p}, τ, c, and the THz beam waist w_0 are taken as free parameters. The first step in our process is to make initial guesses of those parameters. The conductivity is bounded between zero and that of bulk conductivity of gold [14], and the waist is calculated by Gaussian beam method. The second step is to evaluate the complex propagation constant by means of Eqs. (1) and (2) and compute the theoretical complex transmission by Eq. (3). The last step is to compute the error function (Eq. 6) and repeat the step 1 and step 2 until the minimum error value is found. Since many parameters are involved in the process, we use the global optimization algorithm of Matlab to find the global minimum of Eq. (6).

3 Experimental Setup and Samples Preparation

The experimental system is based on standard THz–TDS. The THz emitter is a bare p-type indium arsenide wafer [23] excited by a Ti:sapphire laser at 800 nm and 80 MHz repetition

rate. A photoconductive dipole antenna on gallium arsenide detects the THz wave. The PPWG is placed in the confocal beam waist of four off-axis parabolic mirror system in order to have a nearly frequency-independent focused wave at the waveguide input facet.

Additionally, a combination of wire grid polarizers is placed before and after the waveguide to polarize and to detect the THz beam. A first wire grid polarizer is set before the waveguide input face to provide a parallel or perpendicular polarized input beam, in order to excite either TE or TM waveguide modes. Since the detector is dipole type and can only detect the polarization parallel to the dipole axis, another combination of two wire grid polarizers before the antenna receiver allows us to detect all polarizations of the output THz beam from the waveguide. One wire grid polarizer, placed before the detector, is fixed at an angle 45° to the detector dipole axis. The other wire grid polarizer is placed right after the waveguide output and can be freely rotated to detect horizontal (TE mode) or vertical (TM mode) electric field polarizations.

The waveguide is composed of two flat aluminum plates with 1 mm plate separation, 10 mm length, and 30 mm width. The PPWG is mounted on a stage automatically controlled to scan the entire width of the waveguide (as illustrated in Fig. 1b). The scan is performed perpendicularly to the direction of propagation. The entire experimental setup is held under nitrogen atmosphere in order to avoid water vapor absorption features.

For the dielectric substrate inside the waveguide, we use magnesium oxide (MgO). All substrates have 0.5 mm thickness, 10 mm length, and 30 mm width. We measure the refractive index and the extinction coefficient of MgO by conventional transmission THz–TDS. In the range of 0.1 to 2.2 THz, the refractive index is nearly frequency independent and has a value of 3.15±0.05. Furthermore, THz absorption of MgO is negligible in this spectral range.

Different thicknesses of gold thin film are sputtered onto half of the surfaces of MgO substrates. Four different thicknesses of gold thin film are analyzed here: 1, 4, 8, and 180 nm. The thin film deposition was performed under high vacuum at a rate of 4 nm/min. Atomic force microscopy confirms the measurements of the thickness with ±1 nm surface roughness. A further AFM analysis showed that a network of gold islands and voids is formed on the surface of the substrate for gold thickness less than 8 nm. This formation is quite homogeneous resulting in a smoothness of the surface morphology. The waveguide is assembled with two MgO plates, each 0.5 mm thick, with the gold film located between them, forming a sandwich structure as shown in Fig. 1.

4 Results

A rough measurement of the THz input beam waist is performed first at the maximum electric field during the experiment and the beam is estimated to be around 3 mm. Despite the confocal arrangement of the four parabolic mirrors, the high divergence of the generated THz beam supposes that the waist is frequency dependent. That affects the estimation of power coupling. Therefore, we computed the THz beam waist in function of parabolic mirror focal length following the paraxial beam approximation in Gaussian optics.

In the optimization process, the accuracy of the parameter extraction is mainly affected by the accuracy of experimental setup alignment. The effect of a small variation of sample length and substrate thickness is negligible compared to waveguide misalignment error. Therefore, the reference (through a waveguide containing only two MgO plates) and sample (through a

waveguide containing a thin metal film between two MgO plates) pulses are recorded at five different locations each with 1024 data points and they are averaged in frequency domain. The frequency bandwidth over which the optimization is done is 0.4–1.2 THz. The lower frequency is limited by the PPWG cutoff frequency of the reference, and the higher frequency is limited by the PPWG transmission of the reference signal.

Since the plate separation of the PPWG is 1 mm and the refractive index of the substrate is 3.15, more than 20 modes can propagate in the waveguide for a cutoff frequency at 1.2 THz. However, only odd TE mode (TE_1, TE_3) and even TM modes (TEM, TM_2) can be excited due to the symmetry of the overlap integral in the coupling coefficients. Also, the finite conductivity of the aluminum plates in THz range ($\sigma_r=3.5\times10^5$S/cm) decreases the transmission of higher order modes. For the reference, we include two waveguide modes in the calculation in Eq. (3), while for the sample, we include three modes to account for the measured signals.

figure 2a, b indicates the experimental Fourier transform of the reference (for both TE and TM mode exCitations) along with the THz spectra of the sample waveforms at thicknesses 1, 4, and 8 nm. In both cases, the spectrum of reference and sample overlap at 1 nm film thickness. This indicates that at 1 nm thickness, the gold thin film behaves like an insulator and is indistinguishable from MgO in both configurations. However, as the thickness of the gold film increases, the sample spectra get smaller, indicating the evolution of the dielectric properties of the gold film with increasing thickness.

figure 3a shows the experimental transmission of the waveguide with 180 nm thick gold film, along with the theoretical fitting, in TE mode. The error bar in the figures indicates the alignment error between the five recorded pulses. The best value of fitting for the beam waist is at parabolic mirror focal length around 65 mm in TE mode. Variation of the plasma frequency $\omega_p/2\pi$ between 2000 to 2500 THz yields a similar fit. The scattering time can also change from 10 to 30 fs without changing the fit appreciably. The Drude–Smith parameter c is equal to 0, which means that the gold behaves as a bulk solid with Drude conductivity.

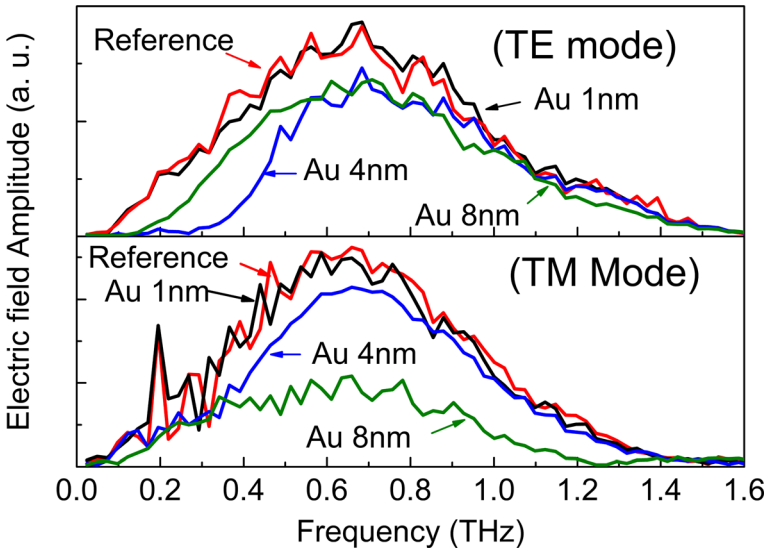

Fig. 2 THz spectra corresponding to reference pulses, gold thin film of thickness 1, 4, and 8 nm inside PPWG in **a** transverse electric mode and **b** transverse magnetic mode

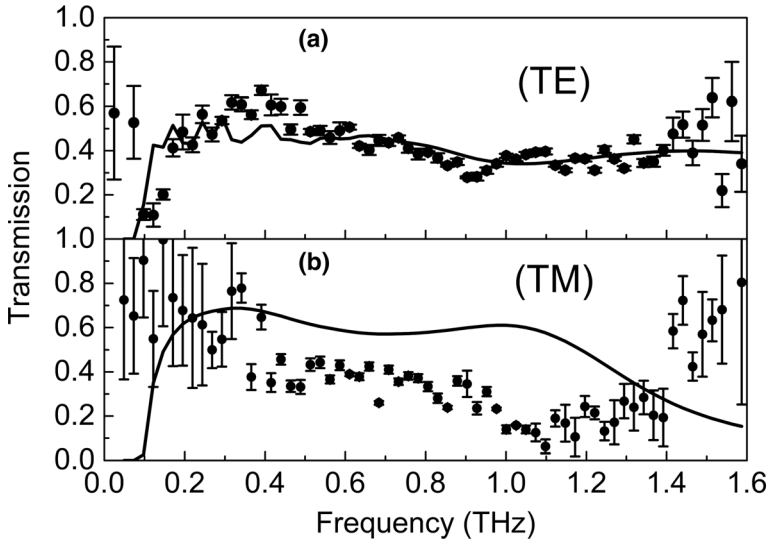

Fig 3 Transmission of gold thin film (thickness=180 nm) in a PPWG. The *solid thick curve* is the theoretical fitting. The *dots* are experimental with error bars. The *theoretical curves* are computed at the value of $\omega_p/2\pi$= 2000 THz and τ=20 fs for **a** TE mode and **b** TM mode

Transmission data and the corresponding theoretical fit for gold 180 nm in TM mode are shown in Fig. 3b. Like in TE mode, the value of the focal length which best fits the experimental data is 65 mm. This fit is obtained with a value of $\omega_p/2\pi$ between 2000 to 2500 THz and τ in the range (10 fs, 50 fs). The parameter c is also 0. It should be noted that the

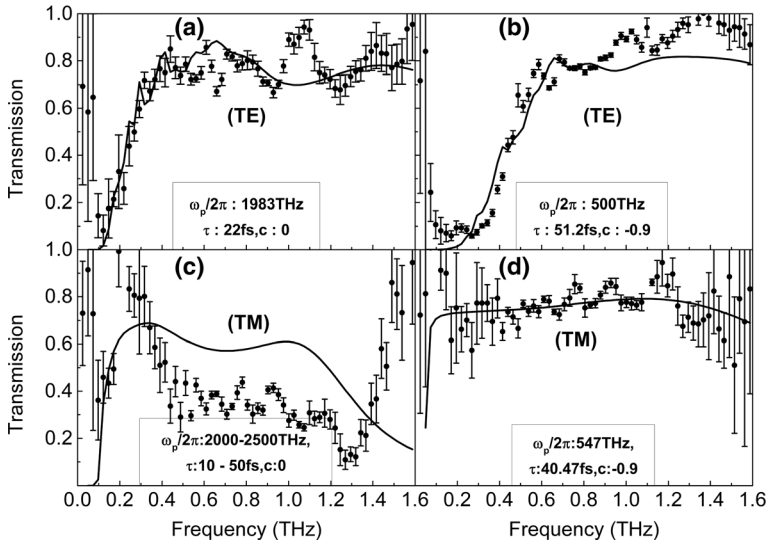

Fig. 4 Transmission of gold thin films in TE mode for gold thin films with thicknesses equal to **a** 8 nm and **b** 4 nm. TM mode for gold thin films: **c** 8 nm and **d** 4 nm. The values in the insets of the figures are the Drude–Smith conductivity parameters

same fitting process is applied for TE and TM mode with their respective characteristic equations.

figure 4 shows the theoretical fitting for gold at thicknesses of 8 and 4 nm for TE and TM modes. For gold at 8 nm thickness, the values of plasma frequency for the best fitting are around the bulk value either in TE or TM mode. The conductivity can be described by Drude model (c=0) with a scattering time a little higher in TM mode fitting. For a 4-nm film thickness, the conductivity changes drastically. The parameter $c \approx -0.9$ and the high scattering time reveal that the gold film is definitely not metallic at this thickness. This is consistent with the results of reference [14], where similar values of Drude–Smith parameters have been calculated for ultrathin layer of gold in the THz range.

5 Discussion

To provide a clear physical interpretation of the results, it is worthwhile to examine the dispersion equations given by Eqs. (1) and (2). When the interface conductivity $\sigma_s \to \infty$, it is easy to see that the dispersion equations reduce to the results for two independent layered PPWGs. The perfectly conductive film partitions the waveguide into two isolated waveguides with half the plate spacing. The phase-matching condition at the interface is no longer valid so that the tangential electric fields across the conductive interface are not continuous. This leads to decoupled equations for two PPWGs. Then, the total electric field detected consists of all possible combinations of excited modes in the lower and upper PPWG, superposed.

In the present work, we assume that the thickest gold film (t=180 nm) has the value of crystalline bulk conductivity [24]. Accordingly, the thickness of the film is nearly three times the skin depth at 1 THz. In this case, the gold thin film could be approximated as a perfect electric conductor and the abovementioned arguments would apply to the data of Fig. 3.

In TE mode, the electric fields of the waveguide containing gold thin film (180 nm) are linear combination of modes symmetrical about the plane $d/2$ with cutoff frequency $f_c = \frac{mc}{2n_{\mathrm{MgO}}\left(d/2\right)}$. ($m$ = 1, 2, 3, …). The dominant mode in each region of the waveguide is also TE_1 with theoretical cutoff frequency f_c=0.095 THz. In the fitting process, different gold conductivities near the bulk value give the same f_c for the dominant and high-order TE mode. It means that the propagation loss is not influenced by the dielectric properties of the gold (which can be considered as perfectly conductive) but only by the THz wave coupling into and out of the waveguide. Therefore, the only free parameter which determines the fit is the frequency-dependent THz beam waist. The value of parabolic mirror focal length extracted for the waist calculation (65 mm) is reasonable since the actual focal length of the mirrors in the experimental setup is 76.2 mm. Also, three modes of the PPWG with the gold thin film are enough to have a good fit (Fig. 3a) since the higher modes coupling coefficients are very small compared to that of the fundamental TE_1 mode.

For the case of TM mode, the presence of a thin metal film extremely perturbs the field distribution relative to the PPWG reference. From Fig. 3b, the fitting curve and the experimental result do not exactly agree. The most obvious reason is that the power coupling of the guided wave with the metallic film is less efficient in TM mode than in TE mode. In addition to the fundamental TEM mode, higher TM modes could be excited. Therefore, the fitting process cannot satisfy the condition required since we only take account of three first higher modes for the sample. We could insert in the analysis model more combination of possible

mode excited to fit the experimental data, but the increasing number of fit parameters renders the analysis less valuable.

When the thickness of the gold film is extremely small ($t<<\delta,\lambda$), the waveguide mode of the upper and lower halves of the waveguide can couple with each other in a symmetric and antisymmetric way. These facts result in hybridization of modes, as described by the dispersion Eqs. (1) and (2). Only modes which satisfy the phase-matching condition propagate down the waveguide. In addition, as in the PPWG reference, the antisymmetric mode cannot couple with the Gaussian input beam.

Despite the fact that gold film which has a thickness of 8 nm satisfies the above condition ($t<<\delta,\lambda$), TE mode again yields a better fit to the analysis than TM mode. In fact, the dispersion equation for TM case is based on the presence of longitudinal E_z field component. In the case of thin metallic sample with finite conductivity, the fundamental mode excited is still the TEM mode that has essentially a vanishing E_z component. The longitudinal current flowing in the film is very small which yields a very low dissipation loss. As a result, the transmission loss is mainly due to the free space coupling to the waveguide at the input and output facets, rather than the propagation loss due to the thin film. This idea is validated by the similarity of the experimental transmission loss for the thin (8 nm) and thick (180 nm) films.

According to Fig. 4a, experimental transmission and the TE mode fitting are in good agreement with the conductivity parameters from reference [14]. Here, the dominant transverse electric fields give two main advantages. First, the distribution of fields remains continuous at the film interface. Even though the conductivity of the gold is still high, a strong coupling through the film keeps the waveguide modes coupled. Second, the concentration of fields in the thin gold layer results in a larger current through the film. A higher energy loss translates into stronger attenuation and thus a larger difference between sample and reference. Unlike in TM mode, the loss in transmission is mainly due to the propagation, not the input and output coupling. Consequently, we can extract spectroscopic information related to the gold film.

In the case of gold thickness at 4 nm, the curve fitting of the transmission in TE and TM modes are in good agreement with the experimental data. The sensitivity of TE mode has been explained in the preceding paragraph and confirmed in the present case. But interestingly, the TM mode analysis also produces a good fit. An explanation for this is that the gold thin film at a thickness of 4 nm induces a very small perturbation of the PPWG reference-dominant TEM mode. Consequently, the power coupling coefficient of the PPWG reference and that of PPWG with thin film is the same. Thus, the optical parameters of the gold could be extracted from the experimental transmission data.

We have also performed conductivity measurements of our samples with the well-established transmission THz–TDS. In summary, the main difference between the PPWG THz–TDS and the standard transmission THz–TDS lies in the fact that the former has a parallel incidence and long wave–sample interaction path, whereas the latter has a normal incidence and very short THz interaction path with the sample. An experimental setup as described in [14] is used for the measurements. Table 1 shows the extracted parameters for optical conductivity with PPWG method and transmission THz–TDS.

The TE mode analysis and the transmission THz–TDS reveal that our gold sample at a thickness of 8 nm has a Drude-like conductivity behavior. In normal THz–TDS, this high conductivity makes the measurement challenging. The low signal to noise ratio for the experimental values induces a large uncertainty in the measurement. However, the agreement between values given by two methods reinforce that TE mode excitation provides the desirable spectroscopic information for conductive thin films.

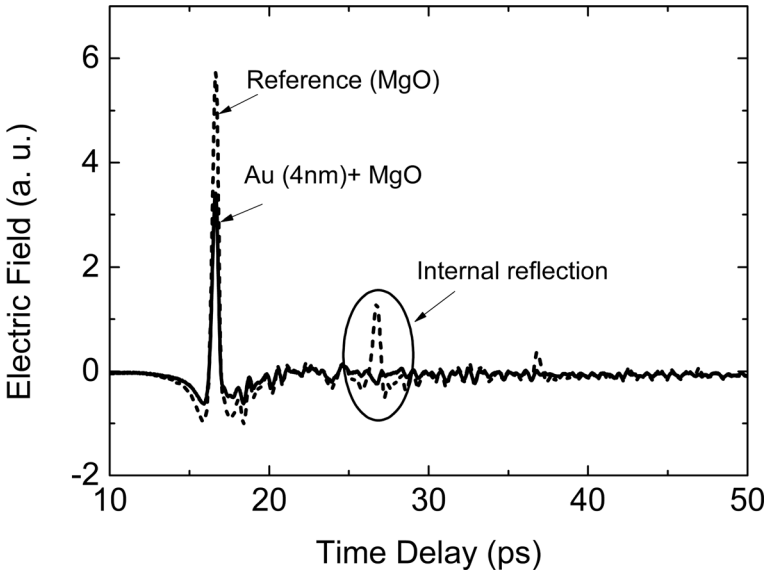

Fig. 5 Time–domain THz waveforms of a transmitted beam through MgO (reference pulse in *dot curve*) and gold 4 nm coating MgO (*solid curve*). The internal reflection pulses are suppressed by gold coating

Finally, a very interesting comparison for both methods is the case of gold thin film at 4 nm. Figure 5 shows the time domain pulse of THz transmitted through MgO coated by 4 nm gold thin film in normal incidence. The suppression of the first reflection pulse indicates that gold thin film behaves like THz antireflection coating. This has been investigated by A. Thoman et al. [25]. Following the same argument as in reference [25], we can draw a simple physical picture to explain the values of conductivity derived for our sample. The antireflection condition is expressed by the following impedance matching $\sigma_s Z_0 = n_{MgO} - 1$. As above, σ_s is the sheet conductivity of gold thin film, while Z_0 is the free space impedance and n_{MgO} is the refractive index of MgO. Since the substrate has negligible extinction coefficient and $n_{MgO} = 3.15$, the impedance matching condition is satisfied if $\sigma_S = 0.0057\ \Omega^{-1}$ (the imaginary part of the conductivity is zero). If we arrange the expression of conductivity (Eq. 8) in real and imaginary part and setting $\mathrm{Im}(\sigma_S)=0$, the value of Drude–Smith conductivity parameters which fulfill the impedance matching condition (with gold thickness 4 nm) is theoretically $c \approx -0.55$ and with DC conductivity $\sigma_0 = \varepsilon_0 \omega_p^2 \tau \approx 2.58.10^6 (\Omega m)^{-1}$. In both transmission and waveguide-based THz–TDS, the plasma frequency and scattering time (cf. Table 1) satisfy approximately the preceding theoretical relation.

Table 1

Drude–Smith parameters	TE mode			TM mode			Transmission THz–TDS	
Gold thickness	4 nm	8 nm	180 nm	4 nm	8 nm	180 nm	4 nm	8 nm
$\omega_p/2\pi$ (THz)	500	1983	[2000, 2500]	547	X	X	341	1629
τ (fs)	51.2	22	[10, 30]	40.4	X	X	70	10
c	−0.9	0	0	−0.9	X	X	−0.35	0

6 Conclusion

In summary, we have analyzed the capability of PPWG to characterize the ultrathin film of conductive material in the THz range. First, it was demonstrated that TE mode excitation offers better sensitivity due to strong transverse electric field which has its maximum in the middle of the waveguide. Second, a good agreement of the optical parameters extracted by TE mode PPWG method and the conventional THz TDS method has been found.

It should be noted that for thin poorly conductive films, TM mode excitation can also be used for a sample located in the middle of PPWG. The requirement is that the thin film does not disturb deeply the electric field distribution of the mode so that perturbation method or the dispersion equation could be employed. However, due to the plasmonic nature of the TM mode [26], we should be careful on the derivation of the right analysis. In addition, a small misalignment or a small air gap between the dielectric slab and the metallic waveguide plates has a drastic effect in the transmission pulse [27].

Acknowledgments This work was supported by JSPS KAKENHI Grant Number 25249049.

References

1. Ren, L. *et al.* Terahertz and Infrared Spectroscopy of Gated Large-Area Graphene. *Nano Lett.* **12,** 3711–3715 (2012).
2. Ge, S. *et al.* Coherent longitudinal acoustic phonon approaching THz frequency in multilayer molybdenum disulphide. *Sci. Rep.* **4,** (2014).
3. Butler, S. Z. *et al.* Progress, challenges, and opportunities in two-dimensional materials beyond graphene. *ACS nano* **7,** 2898–2926 (2013).
4. Gao, W. *et al.* High-contrast terahertz wave modulation by gated graphene enhanced by extraordinary transmission through ring apertures. *Nano Lett.* **14,** 1242–1248 (2014).
5. Sensale-Rodriguez, B. *et al.* Broadband graphene terahertz modulators enabled by intraband transitions. *Nat. Commun.* **3,** 780 (2012).
6. Najmaei, S. *et al.* Vapour phase growth and grain boundary structure of molybdenum disulphide atomic layers. *Nat Mater* **12,** 754–759 (2013).
7. H. Hirori, K. Yamashita, M. Nagai, and K. Tanaka. Attenuated total reflection spectroscopy in time domain using terahertz coherent pulses. *Jpn. J. Appl. Phys.* **43**, L1287 (2004).
8. Zhan, H. *et al.* The metal-insulator transition in VO_2 studied using terahertz apertureless near-field microscopy. *Appl. Phys. Lett.* **91,** 162110–162110–3 (2007).
9. Melinger, J. S., Laman, N., Harsha, S. S. & Grischkowsky, D. Line narrowing of terahertz vibrational modes for organic thin polycrystalline films within a parallel plate waveguide. *Appl. Phys. Lett.* **89,** 251110 (2006).
10. Laman, N., Harsha, S. S., Grischkowsky, D. & Melinger, J. S. High-resolution waveguide THz spectroscopy of biological molecules. *Biophys. J* **94,** 1010–1020 (2008).
11. Zhang, J. & Grischkowsky, D. Waveguide terahertz time-domain spectroscopy of nanometer water layers. *Opt. Lett.* **29,** 1617–1619 (2004).
12. Astley, V., Reichel, K. S., Jones, J., Mendis, R. & Mittleman, D. M. Terahertz multichannel microfluidic sensor based on parallel-plate waveguide resonant cavities. *Appl. Phys. Lett.* **100,** 231108 (2012).
13. Reichel, K. S., Iwaszczuk, K., Jepsen, P. U., Mendis, R. & Mittleman, D. M. *In situ* spectroscopic characterization of a terahertz resonant cavity. *Optica*, **1**, 272-275 (2014).
14. Walther, M. *et al.* Terahertz conductivity of thin gold films at the metal-insulator percolation transition. *Phys. Rev. B* **76,** 125408 (2007).
15. Tsankov, M. A. Permittivity measurement of a thin slab centrally located in a rectangular waveguide. *J. Phys. E: Sci. Instr.* **8,** 963 (1975).
16. Butterweck, H. Mode filters for oversized rectangular waveguides. *IEEE Trans. Microw. Theory Tech.* **16,** 274–281 (1968).
17. Maloney, J. G. & Smith, G. S. The efficient modeling of thin material sheets in the finite-difference time-domain (FDTD) method. *IEEE Trans. Antennas Propag.* **40,** 323–330 (1992).

18. Dressel, M. & Grüner, G. *Electrodynamics of solids: optical properties of electrons in matter*. (Cambridge University Press, 2002).
19. Gallot, G., Jamison, S. P., McGowan, R. W. & Grischkowsky, D. Terahertz waveguides. *J. Opt. Soc. Am. B* **17,** 851–863 (2000).
20. Mendis, R. & Mittleman, D. M. An investigation of the lowest-order transverse-electric (TE 1) mode of the parallel-plate waveguide for THz pulse propagation. *J. Opt. Soc. Am. B* **26,** A6–A13 (2009).
21. Ramo, S., Whinnery, J. R. & Van Duzer, T. *Fields and waves in communication electronics*. (J. Wiley, 1965).
22. Smith, N. V. Classical generalization of the Drude formula for the optical conductivity. *Phys. Rev. B* **64,** 155106 (2001).
23. Liu, K., Xu, J., Yuan, T. & Zhang, X.-C. Terahertz radiation from InAs induced by carrier diffusion and drift. *Phys. Rev. B* **73,** 155330 (2006).
24. Gatesman, A. J., Giles, R. H. & Waldman, J. High-precision reflectometer for submillimeter wavelengths. *J. Opt. Soc. Am. B* **12,** 212–219 (1995).
25. Thoman, A., Kern, A., Helm, H. & Walther, M. Nanostructured gold films as broadband terahertz antireflection coatings. *Phys. Rev. B* **77,** 195405 (2008).
26. Liu, J., Mendis, R. & Mittleman, D. M. The transition from a TEM-like mode to a plasmonic mode in parallel-plate waveguides. *Appl. Phys. Lett.* **98,** 231113 (2011).
27. Mendis, R. Nature of subpicosecond terahertz pulse propagation in practical dielectric-filled parallel-plate waveguides. *Opt. Lett.* **31,** 2643–2645 (2006).